Propagation of spectral functions and dilepton production at SIS energies

Gy. Wolf,[1,*] B. Kämpfer,[2,**] and M. Zétényi[1,***]

[1] *KFKI RMKI, Budapest, Hungary*

[2] *Forschungszentrum Dresden-Rossendorf, Institut für Strahlenphysik, Dresden, Germany*

The time evolution of vector meson spectral functions is studied within a BUU type transport model. Applications focus on ρ and ω mesons being important pieces for the interpretation of the dielectron invariant mass spectrum. Since the evolution of the spectral functions is driven by the local density, the inmedium modifications turn out to compete, in this approach, with the known vacuum contributions.

1. INTRODUCTION

Dielectrons serve as direct probes of dense nuclear matter stages during the course of heavy-ion collisions. The superposition of various sources, however, requires a deconvolution of the spectra by means of models. Of essential interest are the contributions of the light vector mesons ρ and ω. The spectral functions of both mesons are expected to be modified in a strongly interacting environment. Measurements with HADES [1, 2] start to explore systematically the dilepton production at beam energies in the few AGeV region.

Our transport model the time evolution of single particle distribution functions of various hadrons are evaluated within the framework of a kinetic theory. The ρ meson is already a broad resonance in vacuum, while the ω meson may acquire a noticeable width in nuclear matter [3]. Therefore, one has to propagate properly the spectral functions of the ρ and ω mesons. This is the main goal of our paper.

* Electronic address: wolf@rmki.kfki.hu

** Electronic address: b.kaempfer@fzd.de

*** Electronic address: zetenyi@rmki.kfki.hu

2. OFF-SHELL TRANSPORT OF BROAD RESONANCES

Recently theoretical progress has been made in describing the in-medium properties of particles starting from the Kadanoff-Baym equations for the Green functions of particles. Applying first-order gradient expansion after a Wigner transformation [4, 5] one arrives at a transport equation for the retarded Green function. In the medium, particles acquire a selfenergy $\Sigma(x,p)$ which depends on position and momentum as well as the local properties of the surrounding medium. Their properties are described by the spectral function being the imaginary part of the retarded propagator

$$\mathcal{A}(p) = -2\mathrm{I}m\, G^{\mathrm{ret}}(x,p) = \frac{\hat{\Gamma}(x,p)}{(E^2 - \mathbf{p}^2 - m_0^2 - \mathrm{R}e\,\Sigma^{\mathrm{ret}}(x,p))^2 + \frac{1}{4}\hat{\Gamma}(x,p)^2}\,, \tag{1}$$

where the resonance widths Γ and $\hat{\Gamma}$ are related via $\hat{\Gamma}(x,p) = -2\mathrm{I}m\,\Sigma^{\mathrm{ret}} \approx 2m_0\Gamma$, and m_0 is the vacuum pole mass of the respective particle.

To solve numerically the Kadanoff-Baym equations one may exploit the test-particle ansatz for the retarded Green function [4, 5]. This function can be interpreted as a product of particle number density multiplied with the spectral function $\mathcal{A}$.

The relativistic version of the equation of motion have been derived in [4]:

$$\frac{d\mathbf{x}}{dt} = \frac{1}{1-C}\frac{1}{2E}\left(2\mathbf{p} + \boldsymbol{\nabla}_p \mathrm{R}e\,\Sigma^{\mathrm{ret}} + \frac{m^2 - m_0^2 - \mathrm{R}e\,\Sigma^{\mathrm{ret}}}{\hat{\Gamma}}\,\boldsymbol{\nabla}_p\hat{\Gamma}\right), \tag{2}$$

$$\frac{d\mathbf{p}}{dt} = -\frac{1}{1-C}\frac{1}{2E}\left(\boldsymbol{\nabla}_x \mathrm{R}e\,\Sigma^{\mathrm{ret}} + \frac{m^2 - m_0^2 - \mathrm{R}e\,\Sigma^{\mathrm{ret}}}{\hat{\Gamma}}\,\boldsymbol{\nabla}_x\hat{\Gamma}\right), \tag{3}$$

$$\frac{dE}{dt} = \frac{1}{1-C}\frac{1}{2E}\left(\partial_t \mathrm{R}e\,\Sigma^{\mathrm{ret}} + \frac{m^2 - m_0^2 - \mathrm{R}e\Sigma^{\mathrm{ret}}}{\hat{\Gamma}}\,\partial_t\hat{\Gamma}\right), \tag{4}$$

with the renormalization factor

$$C = \frac{1}{2E}\left(\partial_E \mathrm{R}e\,\Sigma^{\mathrm{ret}} + \frac{m_n^2 - m_0^2 - \mathrm{R}e\Sigma^{\mathrm{ret}}}{\hat{\Gamma}}\partial_E\hat{\Gamma}\right). \tag{5}$$

In the above, $m = \sqrt{E^2 - \mathbf{p}^2}$ is the mass of an individual test-particle. The selfenergy Σ^{ret} is considered to be a function of density n, energy, and momentum.

The change of the test-particle mass m can be more clearly seen combining Eqs. (3) and (4) to

$$\frac{dm^2}{dt} = \frac{1}{1-C}\left(\frac{d}{dt}\mathrm{R}e\,\Sigma^{\mathrm{ret}} + \frac{m^2 - m_0^2 - \mathrm{R}e\,\Sigma^{\mathrm{ret}}}{\hat{\Gamma}}\,\frac{d}{dt}\hat{\Gamma}\right) \tag{6}$$

with the comoving derivative $d/dt \equiv \partial_t + \mathbf{p}/E\boldsymbol{\nabla}_x$. This equation means that the square of the particle mass tends to reach a value shifted by the real part of the selfenergy within a

range of the value of $\hat{\Gamma}$. Thus, the vacuum spectral function is recovered when the particle leaves the medium.

The equation of motions of the test-particles have to be supplemented by a collision term which couples the equations for the different particle species. It can be shown [5] that this collision term has the same form as in the standard BUU treatment.

In our calculations we employ a simple form of the selfenergy of a vector meson V:

$$\mathrm{Re}\,\Sigma_V^{\mathrm{ret}} = 2m_V \Delta m_V \frac{n}{n_0}, \tag{7}$$

$$\mathrm{Im}\,\Sigma_V^{\mathrm{ret}} = m_V \left(\Gamma_V^{\mathrm{vac}} + \frac{n v \sigma_V}{\sqrt{1-v^2}} \right). \tag{8}$$

Eq. (7) causes a "mass shift" $\Delta m = \sqrt{m_V^2 + \mathrm{Re}\,\Sigma_V^{\mathrm{ret}}} - m_V$ characterized by Δm_V and roughly being proportionally to the density n of the surrounding matter. The imaginary part contains the vacuum width Γ_V^{vac}. The second term in Eq. (8) results from the collision broadening.

If a ρ meson is generated at normal density its mass is distributed in accordance with the spectral function. If the meson propagates into a region of higher density then the mass will be lowered according to the action of $Re\Sigma^{\mathrm{ret}}$ in Eq. (6). However if the meson comes near the threshold the width $\hat{\Gamma}$ becomes very small and the second term of the right hand side of Eq. (6) dominates, so reverses this trend leading to an increase of the mass.

In Fig. 1 we show how the masses of test-particles for ω mesons are developing in a heavy ion collisions. For the end of the collisions the masses reach the vacuum value fulfilling our main expectations.

3. DIELECTRON PRODUCTION

The dielectrons come from different sources, the detailed description can be found in [6–8]. Direct vector meson decays $V \to e^+e^-$ is calculated by integrating the local decay probabilities along their trajectories.

We also include into our simulations a bremsstrahlung contribution which is guided by a one-boson exchange model adjusted to pp virtual bremsstrahlung and transferred to pn virtual bremsstrahlung [9].

An essential dielectron contribution comes from the Dalitz decay of the π^0, η, ω mesons and the excited baryonic resonances emitting a dielectron together with a photon [10].

The bremsstrahlung contribution and the Dalitz decay of baryon resonances are very uncertain [8].

On the left panel in Fig. 2 we compare our calculations with the HADES data. The agreement is very good. On the right panel we show the result with vacuum spectral function and with the dotted line the total cross ection calculated with in-medium vector mesons. The difference is very small giving no hope to observe these medium effects on the vector mesons in the dilepton spectra for light systems. However, for heavy systems the difference is larger, giving a reasonable chance for observing it.

ACKNOWLEDGMENTS

We acknowledge the continuous information by the HADES collaboration. The work is supported by the BMBF 06DR121, 06DR136, GSI and OTKA T71989.

---

1. G. Agakichiev *et al.* (HADES collaboration), Phys. Rev. Lett. **98**, 052302 (2007).
2. G. Agakichiev *et al.* (HADES collaboration), Phys. Lett. B **663**, 43 (2008).
3. Gy. Wolf, B. Friman, M. Soyeur, Nucl. Phys. A **640**, 129 (1998).
4. W. Cassing, S. Juchem, Nucl. Phys. A **672**, 417 (2000).
5. S. Leupold, Nucl. Phys. A **672**, 475 (2000).
6. Gy. Wolf *et al.*, Nucl. Phys. A **517**, 615 (1990).
7. Gy. Wolf, W. Cassing, U. Mosel, Nucl. Phys. A **552**, 549 (1993);
   S. Teis *et al.*, Z. Phys. A **356**, 421 (1997).
8. H. W. Barz, B. Kampfer, Gy. Wolf, M. Zetenyi, The Open Nuclear and Particle Physics Journal **3**, 1 (2010).
9. L. P. Kaptari, B. Kämpfer, Nucl. Phys. A **764**, 338 (2006).
10. M. Zétényi, Gy. Wolf, Phys. Rev. C **67**, 044002 (2003).

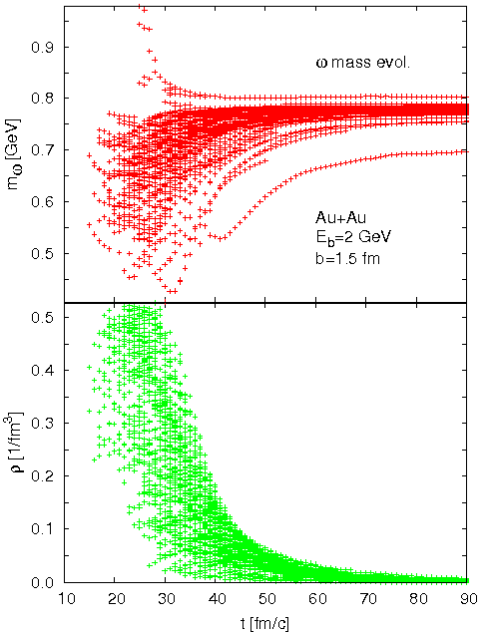

Figure 1. Time evolution of the masses of several test-particles of ω mesons in a central AuAu collision at 2 AGeV kinetic beam energy at an impact parameter of 1.5 fm. In the lower panel we show the corresponding densities experiencing by the ω's.

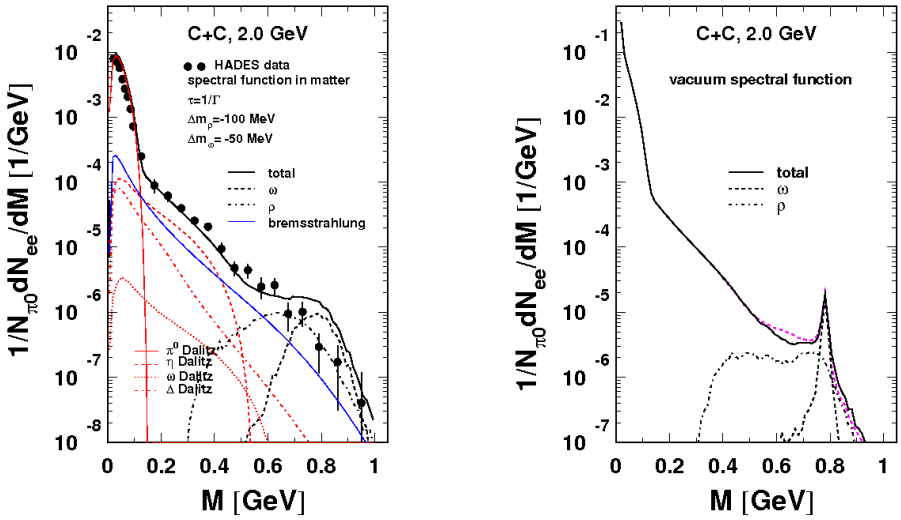

Figure 2. Dielectron invariant mass spectra for C(2 AGeV) + C calculated with the inmedium spectral function. The various sources of the dielectron invariant mass spectrum are indicated. Right panel shows the spectra after applying the experimental filter compared to HADES data [1].

FIGURE CAPTIONS

Fig. 1: Time evolution of the masses of several test-particles of ω mesons in a central AuAu collision at 2 AGeV kinetic beam energy at an impact parameter of 1.5 fm. In the lower panel we show the corresponding densities experiencing by the ω's.

Fig. 2: Dielectron invariant mass spectra for C(2 AGeV) + C calculated with the inmedium spectral function. The various sources of the dielectron invariant mass spectrum are indicated. Right panel shows the spectra after applying the experimental filter compared to HADES data [1].